Magnetic Polymer Chains of Iron and Zwitterionic Quinoidal Ligands on the Ag(111) Surface

Hassan Denawi, Elena Nardi, Mathieu Koudia, Olivier Siri, Mathieu Abel, Roland Hayn

To cite this version:

Hassan Denawi, Elena Nardi, Mathieu Koudia, Olivier Siri, Mathieu Abel, et al.. Magnetic Polymer Chains of Iron and Zwitterionic Quinoidal Ligands on the Ag(111) Surface. Journal of Physical Chemistry C, 2019, 124 (2), pp.1346-1351. 10.1021/acs.jpcc.9b08209 . hal-03096953

HAL Id: hal-03096953
https://hal.science/hal-03096953

Submitted on 5 Jan 2021

Magnetic Polymer Chains of Iron and Zwitterionic Quinoidal ligands on the Ag(111) Surface

Hassan Denawi [1, *], *Elena Nardi* [1], *Mathieu Koudia* [1], *Olivier Siri* [2] *Mathieu Abel* [1]*and Roland Hayn* [1]

[1]Aix Marseille Université, CNRS, IM2NP UMR 7334, 13397, Marseille, France.

[2]Aix Marseille Université, CNRS, CINAM, UMR 7325, Campus de Luminy, 13288, Marseille, France.

ABSTRACT

On-surface polymerization of iron atoms and zwitterion quinone (ZQ) molecules on Ag(111) is studied experimentally under ultra-high vacuum and theoretically in the framework of density functional theory . The resulting one-dimensional (1D) polymer chain is a promising model system to study both magnetic and conductive properties in one dimension. Previously we have shown that such polymer synthesis is possible over large scale by a controlled co-deposition of the two elements (i. e. metal and molecule) on a Ag(111) substrate (Nano Res. **2017**, 10, 933). In that case, polymer chains are bound together to form a two-dimensional (2D) arrangement of spin chains influencing the magnetic properties of individual chains. Here we show that individual chains can be obtained using a sequential deposition of first metals and then ligands by scanning tunnelling microscopy on the Ag(111) surface. Ab-initio calculations are used to compare the atomic, electronic and magnetic structures of isolated Fe-ZQ polymer chains (1D) to the previously obtained two dimensional (2D) arrangement of the polymer chains. The adsorption energy is determined using the spin-polarized generalized gradient approximation (SGGA) and the SGGA+U approximation. It yields small values of less than 530 meV per Fe. On the Ag(111) surface, the most favourable adsorption site of Fe in the polymer chain is the hexagonal-close-packed (hcp) site for the 1D polymer but it changes to the face-centred-cubic (fcc) site for the 2D polymer. Using both SGGA and SGGA+U methods, we find a small difference between the two sites: face-centred-cubic (fcc) and hexagonal-close-packed (hcp). This latter is the most stable adsorption energy when we add the Hubbard U term to the SGGA method.

INTRODUCTION

Conductive metal-organic frameworks (c-MOFs) emerged recently as promising candidates in many different application fields as they offer unique possibilities to combine conductive properties, [1,2] magnetic properties [3–6] and catalytic properties. [7] Especially the prospective of electrical conductivity in MOF's attracted recently a lot of attention to these systems in nanotechnology. [8–10] Many studies have shown that these materials are very good candidates for use in devices for electrocatalysis, [7,11–14] fuel cells, [11,15] and chemical sensing. [16–18] when synthetized in layered materials. The great originality of these MOF conductive materials with respect to the insulating MOFs comes from a strong hybridization of the orbitals of the metal centers with the orbitals pi of the organic molecules giving them good conduction properties. At the same time, it imposes a state of oxidation II of the metal centers responsible for the catalytic properties but also of the magnetic properties in networks whose architecture is dictated by the organic ligand. Thanks to that it has been possible to synthesize 1D conductive MOF including magnetic atoms. 1D magnetic chains are interesting for several reasons. First of all, they would allow crucial experiments to answer fundamental questions on low-dimensional spin systems. [19,20] Second, they are interesting in the field of spintronics, where not only the electron charge but also its spin is used for information processing. And third, spin chain systems are discussed for many possible spintronics applications, going from magnetic memories up to quantum computing. [4,5]

Recently, it was shown that zwitterionic quinoidal molecules and metallic Fe can form, after adsorption on Ag(111) or Au(110) surfaces, a well ordered arrangement of spin chains up to micrometer. [6,21] The STM and LEED measurements in connection with a theoretical analysis of the obtained polymer adsorption on Au(110) [6] indicate that the adsorbed polymers adapt their lattice constants to the underlying substrate. Surprisingly, the polymer lattice constants on Au(110) and Ag(111) substrates differ by 6 per cent and such a large difference can eventually be explained by two nearly degenerate energy minima for different lattice constants corresponding to two different spin states (S=1 or S=2) as expected for spin crossover compounds. [6]

However, previous theoretical studies were either focused on the electronic and magnetic structures of free polymers [3] or treated just the adsorption on the Au(110) substrate. [6] Experimentally, only the 2D arrangement of Fe-ZQ polymer chains were reported. On the other hand, the ab-initio study of isolated free polymers indicated very interesting perspectives for these new systems, intimately related to their one dimensionality.

In the present communication, we report on two advances with respect to published work. [3,6,21] First of all, the on-surface synthesis of isolated magnetic polymer chains obtained by sequential deposition and, second, a detailed theoretical analysis of the adsorption of 1D and 2D Fe-ZQ polymers on Ag(111) detailing the adsorption process and the resulting atomic, electronic and magnetic properties. Finally, electronic structure calculations allow the determination of the density of states which informs on the charge transport efficiency.

EXPERIMENTAL METHODS

The zwitterionic quinoidal ligand was prepared as described in the literature. [22,23] All experiments were performed in a multi-characterization chamber under ultra-high vacuum (UHV). Zwitterion molecules were evaporated from a crucible held at 430 K. Fe atoms were deposited from an iron rod (Goodfellow) using an electron-beam evaporator. The experiments are done with a molecular deposition rate of 0.05 ML·min^{-1} calibrated at room temperature. The resulting synthetic films were characterized using room-temperature scanning tunneling microscopy (Omicron VT-STM). Images were plane-corrected and analysed using the WSxM software.

THEORETICAL METHOD

To determine the electronic and magnetic properties of the systems, within the framework of density functional theory (DFT) periodic calculations were performed using the Vienna Ab initio Simulation Package (VASP), [24–26] in the spin polarized generalized gradient approximation with an explicit inclusion of the Hubbard U term correction (SGGA+U) of Perdew and Wang (PW91), [27,28] for the exchange and correlation potential and the Projector Augmented Wave (PAW) pseudo potentials. [25–30] The Coulomb correlation in the d shell was taken into account by a Hubbard term in the form proposed by Liechtenstein et al. [31] The necessity of the SGGA+U method for metal-organic compounds with transition metal ions is proven by many examples as TM-ZQ, [3,6] TM-TCNB [32] or TM-Pc [32,33] where TM is a transition metal. The correlation energy (U) of 4 eV and exchange energy of J = 0.90 eV is taken for the Fe d orbitals. To study the polymer on the surface we use a kinetic-energy cutoff of 480 eV and the convergence criteria for the electronic step was set to 10^{-4} eV. The structure was relaxed until the residual forces were smaller than 0.02 eV/Å and we used a first order Methfessel-Paxton setting with a smearing (SIGMA) of 0.2 eV. The method of Methfessel-Paxton also results in a very accurate description of the total energy. Only a single k-point, namely the Γ-point, was used. The substrate is simulated by a 5-layer Ag (111) surface onto which we add the Fe-ZQ layer. The separation distance between the slabs (top vacuum) is set to 10 Å. It was verified that greater separation distances did not lead to significantly lower energies. The free standing polymer without surface was relaxed until the residual forces were 10^{-6} eV/Å and the convergence criteria for energy was 10^{-7} eV. The Brillouin zone was sampled by a k-point set of (8×1×1) for the one-dimensional (1D) free standing polymer and by a k-point set of (8×5×1) for the 2D arrangement without substrate using the Monkhorst-Pack k-point mesh. [34] Figure 1 shows the atomic structure of Fe-ZQ on Ag(111) after relaxation in the most stable configuration.

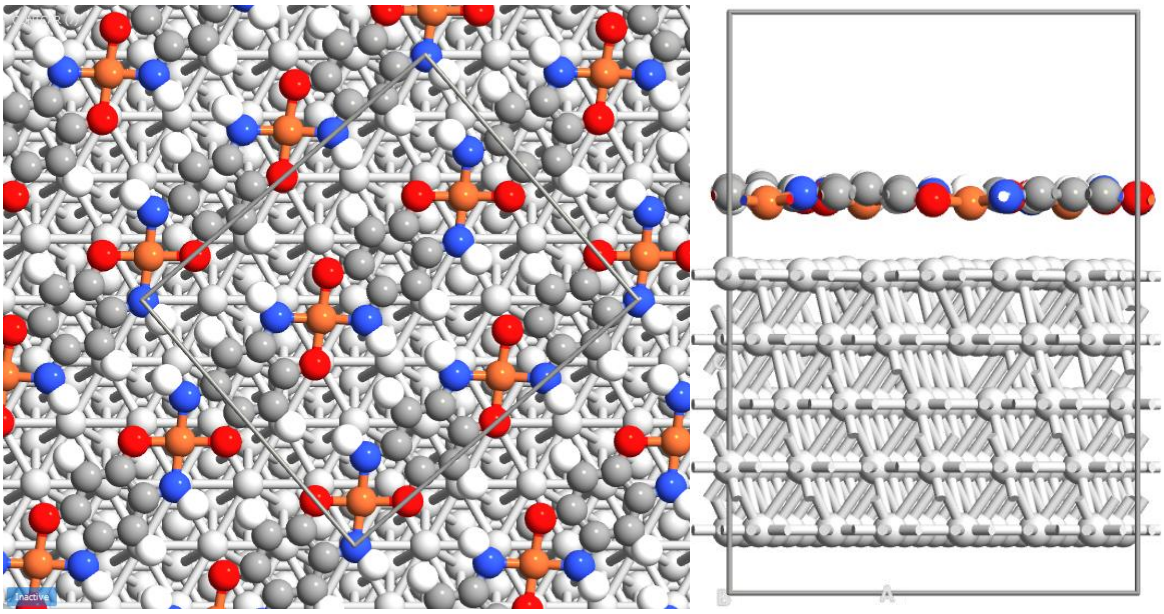

Figure 1: Schematic representation of the 2D Fe-zwitterionic quinone on Ag(111)- $\left(\sqrt{7}\,x\,\sqrt{7}\right)\,R19°$ ***surface. The Fe atoms are in the hexagonal-close-packed (hcp) site, with the method SGGA+U and U = 4 eV. Left: top view, Right: side view.***

RESULTS AND DISCUSSION

On-surface synthesis under UHV is a promising strategy for controlling matter at the atomic level, with important implications for the design of new one- and two-dimensional materials having remarkable electronic and magnetic properties. First, we investigate the behavior of the selected system composed by iron atoms and ZQ molecules on Ag(111). Figures 2a, b, and c are obtained after sequential deposition of iron atoms on the Ag(111) substrate maintained at room temperature, the sample is heated to 170°C and the molecules are deposited on the Fe/Ag(111) substrate. Step edges are decorated with Fe islands of several hundreds of atoms, of about 5 nm × 5 nm × 0.8 nm. Then the additional deposition of molecules allows the formation of needles which are 40-100 nm long and have a width of 2 nm. These needles grow on the terraces between the step edges by incorporation of Fe atoms (coming probably from the Fe islands) in between the ZQ molecules. They are composed at its periphery by 2 wires with protrusions of 7.6 Å periodicity that are compatible with the formation of 1D polymers. Between these two wires, one can observe the formation of a complex composed by a central iron atom and two ZQ molecules that is schematically shown in Figure 1d. These results clearly demonstrate the efficiency of the method, which consists of deposition of iron atoms and molecules on an Ag (111) substrate.

Figures 2e and 2f are obtained as previously reported[21] by co-deposition of Fe atoms and molecules on the substrate maintained at 250°C. 1D polymeric wires with protrusion separated by 7.6 Å are stacked to form two-dimensional (2D) networks. The co-deposition of quinoid zwitterion molecules with iron atoms on an Ag (111) surface allows the formation of micrometer-sized 2D materials based on covalent coordination bonds. The structural arrangement at the atomic level is investigated by scanning tunneling microscopy (STM).

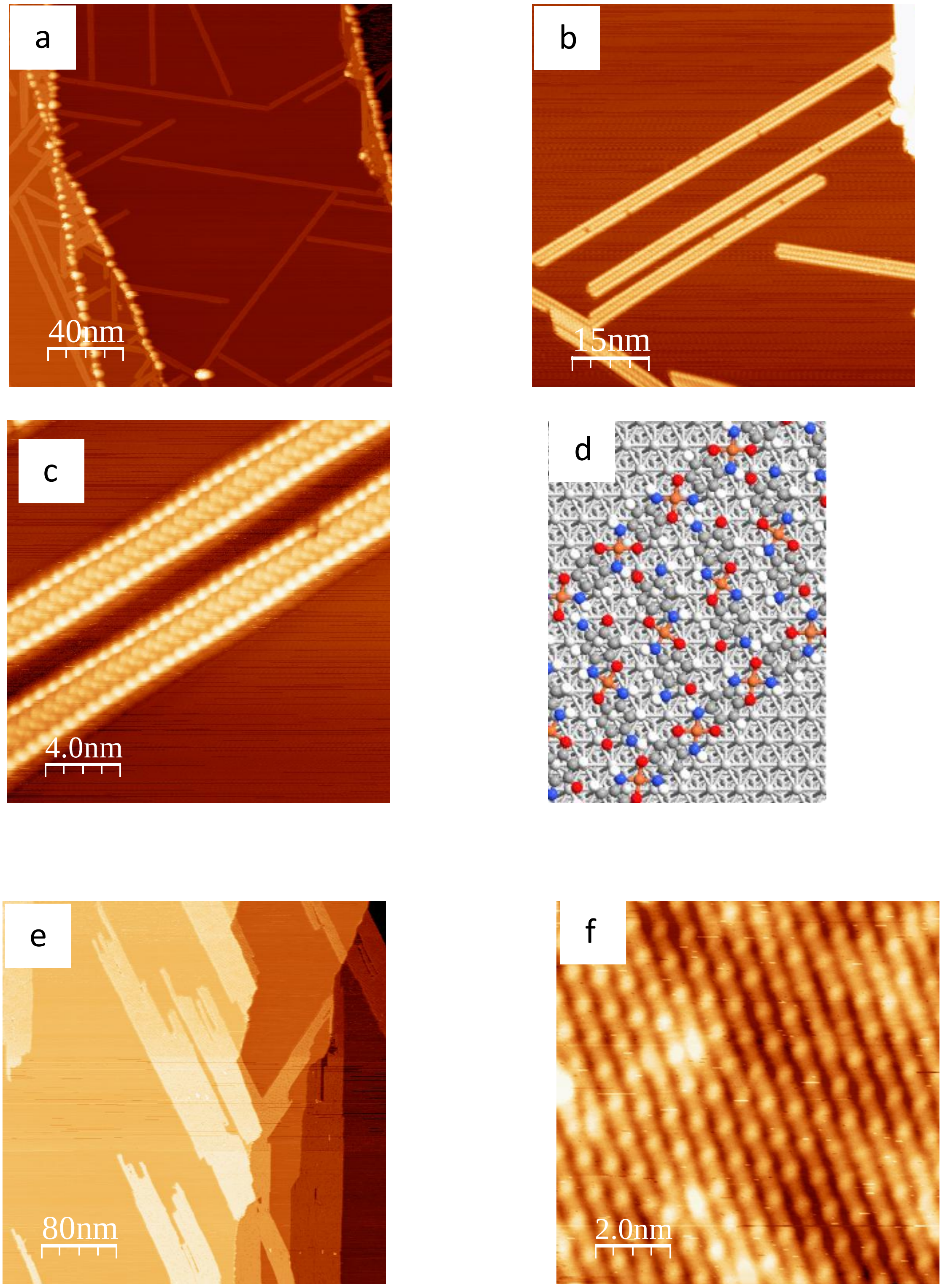

Figure 2: (a, b and c) STM images polymeric chains obtained after sequential deposition of iron atoms on Ag(111) kept at room temperature then the sample is heated to 170°C and zwitterion molecules are deposited , (d) schematic representation of the Fe-zwitterionic quinone and (e and f) STM topography of co-deposited Fe atoms and zwitterionic quinone on the Ag (111) surface heated at 250°C.

In both cases of sequential deposition and co-deposition, the chains are oriented at ±20° from the close-packed direction of the substrate with a periodicity of 7.6 Å. It is important to note that within an individual chain, there is no modulation of the height of the polymer, indicating equivalent adsorption sites for all the Fe atoms. The only difference between co-deposition and sequential deposition is the packing of the polymer chains. A (√7x√7) R19° epitaxial relationship is obtained in the case of co-deposition whereas individual chains separated by molecules are obtained in the case of sequential deposition. The lattice parameters used in calculations are set in agreement with this epitaxial relationship. For the two-dimensional free-standing polymer (2D) the values of a and b are 15.30 Å and 13.24 Å, respectively, and the total magnetic moment is 2 μ_B per Fe. The local magnetic moment is 2.06 μ_B (1.94 μ_B) for each Fe site corresponding to S = 1 for the SGGA (SGGA+U) methods, respectively, see Table 1.

Table 1. Lattice constants (a and b) in (Å), Magnetic Moments per Unit Cell M, and Local Magnetic Moments per Fe (M_d) at Fe Site for the free-standing polymer.

	METHOD	a and b (Å)	M (μ_B)	M_d (μ_B)
1D	SGGA	a = 15.3	4	2.064
	SGGA+U	a = 15.3	4	1.951
2D	SGGA	a = 15.3 b =13.24	8	2.062
	SGGA+U	a = 15.3 b = 13.24	8	1.946

The objective is the study of the adsorption phenomena constituted by the Fe-ZQ polymer adsorbed on the noble metal surface Ag (111). From these calculations we derive the following trends in adsorption energies, geometric, electronic and magnetic structure. As mentioned above, there is strong experimental evidence that Fe-ZQ polymers adsorb on Ag(111) surface with high coverage under typical polymer deposition conditions. The length of the linear chains and the coverage increase with the quantity of Fe atoms. [21] To investigate the interaction with the substrates, geometry optimizations were carried out where the Fe atoms were placed over different sites, the top (T), bridge (B), hexagonal-close-packed (hcp) or face-centered-cubic (fcc) sites on the first layer Ag(111) as illustrated in Figure 1. The adsorption energy for Fe-ZQ on the surface is defined as $E_{ads} = E_{polymer/surface} - E_{surface} - E_{polymer}$. This value is confirmed by total energy calculations using spin polarized Generalized Gradient Approximation (SGGA) and inclusion of the Hubbard U term correction. The adsorption energies, total and local magnetic moments and geometric parameters of different configurations of the selected adsorption configurations were calculated (see Table 2 and 3). The adsorption energy for the stable adsorption site corresponds to the absolute minimum of the molecule moving on the surface. First, it is clear from Table 2 that the SGGA and SGGA+U methods give different results for the adsorption energy E_{ads} and the total magnetic moment. The hexagonal-close-packed (hcp) site is the most favorable one in the case of 1D Fe-ZQ polymer on surface Ag (111). The Fe−O (Fe−N) bond length d_{Fe-O} (d_{Fe-N}) of the polymer on adsorption was calculated to be 1.88 (1.87) Å for the SGGA method. While the d_{Fe-O} (d_{Fe-N}) length increases in the SGGA+U method, d_{Fe-O} (d_{Fe-N}) rises from 1.88 to 1.91 Å (1.87 to 1.90 Å) respectively. The vertical distance between a Fe atom and the Ag(111) substrate, i.e. the adsorption height Fe-Ag(111) is 2.58 Å (2.68 Å) within the SGGA (SGGA+U) method, the distance between the irons atoms (Fe-Fe) is 7.65 Å for the ferromagnetic (FM) configuration. The adsorption energy for the most stable adsorption configuration is -0.525 eV (-0.263 eV) per Fe atom. The total magnetic moment M is 1.74 μ_B (1.93 μ_B) and the local magnetic moment is 1.89 μ_B (1.96 μ_B) per Fe, when we use the SGGA (SGGA+U) method, see Table 2. On the other hand, the face-centred-cubic (fcc) site is the most favorable one for the 2D Fe-ZQ polymer on the surface Ag (111). However, it should be mentioned that the variation between the two different sites face-centred-cubic (fcc) and hexagonal-close-packed (hcp) is very small of only 1 … 3 meV as shown in Table 2. The adsorption energy for the most stable ferromagnetic configuration is -0.351 eV (-0.175 eV) for the SGGA (SGGA+U) method. The total magnetic moment of M = 1.90 μ_B in the SGGA is smaller than M = 2.01 μ_B in SGGA+U method. Not surprisingly, for both configurations, SGGA gives the largest adsorption energy and smallest adsorption height. SGGA+U is a very popular functional, widely used in adsorption studies. Here SGGA+U gives an E_{ads} of -0.175 eV, with the difference in adsorption energy between the two configurations (1D and 2D) being only 0.091 eV per Fe atom. It can also be noticed that, for the Fe-ZQ, the energy difference between two configurations with the fcc and hcp adsorption sites is ~1-3 meV, which suggests that these two configurations are equivalent at room temperature Present calculations show that the Fe-ZQ polymer is adsorbed at the hcp site on the Ag(111) surface. The distances between metal ions (Fe) and Ag surface in the configurations with the lowest total energy are 2.62, and 2.66-3.52 Å for the cases of 2D Fe-ZQ polymers, without and with the Hubbard U correction, respectively.

Table 2. Adsorption energies E_{ads} in eV for different sites of the Fe-ZQ on the Ag (111), distances between the central Fe atoms and the Ag surface are provided ($d_{Fe\text{-}Ag}$, in Å), total magnetic moments (M per Unit Cell, in μ_B), local magnetic moments of the d orbital at the TM atoms (M_d per TM atom, in μ_B) for different sites of the Fe-ZQ on the Ag (111) with the SGGA and SGGA+U (U = 4 eV) methods.

Fe-ZQ/Ag(111)			Top	Bridge	Hcp	fcc
SGGA	1D	E_{ads}	-0.396	-0.399	-0.525	-0.523
		$d_{Fe\text{-}Ag}$	2.78	2.67	2.58	2.51
		M	3.481	3.505	3.482	3.452
		M_d	1.977;1.945	1.937;1.910	1.893;1.890	1.880;1.892
	2D	E_{ads}	-0.288	-0.266	-0.350	-0.351
		$d_{Fe\text{-}Ag}$	2.84	2.75	2.62	2.64
		M	7.334	7.556	7.582	7.576
		M_d	1.937-1.951	1.941-1.948	1.910-1.934	1.920-1.932
SGGA+U	1D	E_{ads}	-0.183	-0.162	-0.263	-0.262
		$d_{Fe\text{-}Ag}$	2.86	2.82	2.68	2.68
		M	4.266	4.248	3.851	3.840
		M_d	1.957;1.955	1.968;1.963	1.963;1.955	1.964;1.953
	2D	E_{ads}	-0.156	-0.151	-0.172	-0.175
		$d_{Fe\text{-}Ag}$	2.87-3.87	2.82-3.89	2.66-3.52	2.75-3.67
		M	8.447	8.169	8.055	8.190
		M_d	1.933-2.013	1.936-2.020	1.940-2.032	1.939-2.030

Since we are interested in the magnetic properties of the systems, the spin-polarized density of states projected on the Fe(II) in the adsorbed polymer with the lowest energy configurations is presented in Figure 3a-b to identify the influence of the Ag surface on the electronic structures of the adsorbates. First of all, the DOS in Fig. 3 looks very similar to the DOS of a free standing chain (not shown) besides a certain smearing of the peaks. Also the position of the Fermi level is almost not shifted showing the absence of any charge transfer between substrate and polymer chain. The electronic structure provides deep insight into the interaction between adsorbate and surface. We now analyze the partial densities of states (PDOS) of the Fe-ZQ polymer on Ag(111). The peak at +0 eV in the SGGA method (Figure 3a) has been shifted to -1.0 eV for the SGGA+U method. In the spin up channel, all peaks are shifted closer to the Fermi level. We observe that the spin-down d_{xy} and the d_{z^2} orbitals are completely filled, leaving $d_{x^2-y^2}$ empty for the spin-up as shown in Figure 3 and giving a magnetic moment close to 2 μ_B per Fe (S = 1).

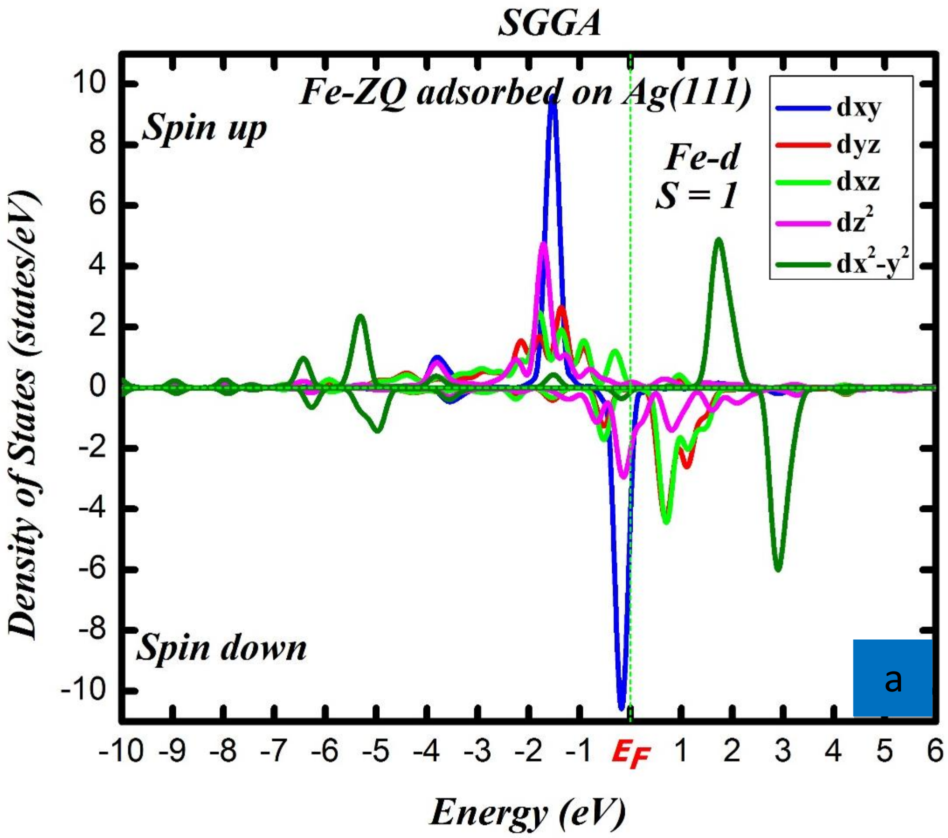

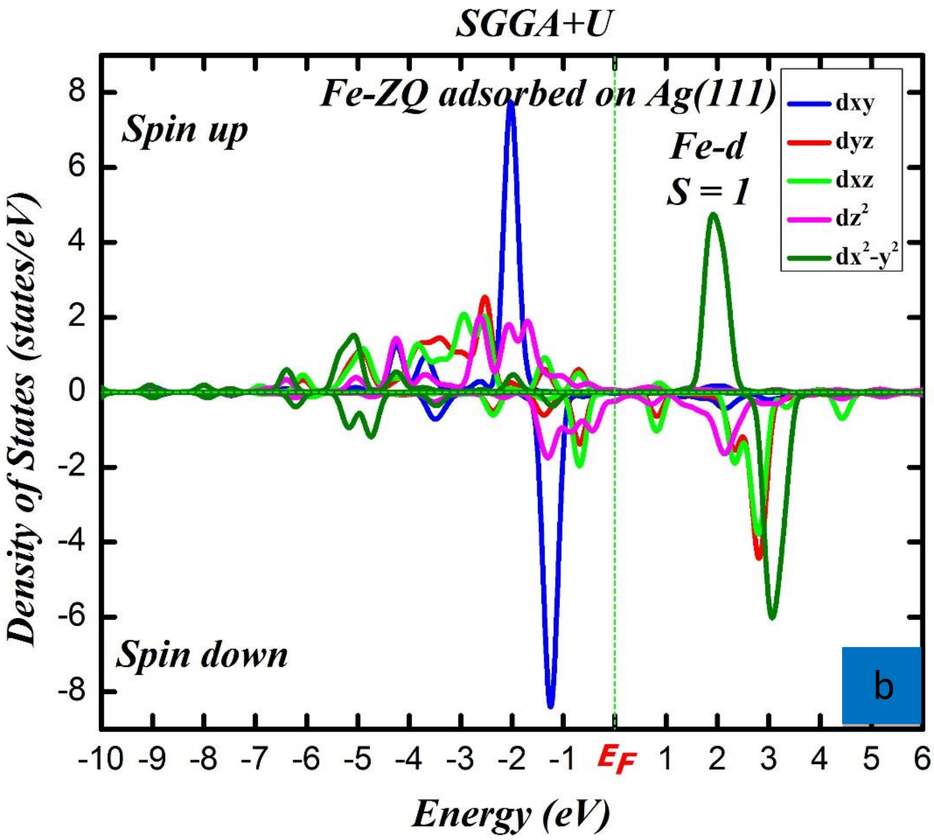

Figure 3: (a and b) PDOS of the Fe-3d states in the 2D Fe-ZQ on the Ag (111) surfaces obtained from the PAW-SGGA and PAW-SGGA+U respectively.

CONCLUSIONS

The conclusion that can be drawn is that the adsorption, electronic, and magnetic structure of Fe-ZQ (1D and 2D) adsorbed on Ag (111) surfaces have been obtained by the modification of the growth conditions. 1D isolated polymer chains are obtained by sequential deposition of Fe followed by ZQ deposition whereas 2D close-packed arrangements are obtained by co-deposition of the two precursors Fe and ZQ. These two configurations (1D and 2D) together with the underlying substrate had been systematically studied using the SGGA and the SGGA+U approximations within DFT calculations. The hexagonal-close-packed (hcp) and face-centred-cubic (fcc) site are the most favorable ones for the adsorption of Fe-ZQ on the Ag (111) surfaces. We have calculated the partial density of states of the Fe-3d states for the Fe-ZQ/Ag (111) system, as well as the distance between the atoms (Fe-Fe, Fe-N, Fe-O and Fe-Ag). Above all, our results based on electronic structures can give reasonable explanations and predictions on the existing experimental results from a theoretical level. We have shown a way to synthesize well separated magnetic chains with antiferromagnetic nearest neighbour exchange interaction [3,6] on a metallic substrate. This new strategy will hopefully open a way to study experimentally that well-known model system of low-dimensional physics.

AUTHOR INFORMATION

Corresponding Author

*E-mail: hassan.denawi@im2np.fr (H.D.).

ACKNOWLEDGEMENTS

This work was supported by the Computer resources of the Centre Informatique National de l’Enseignement Supérieur (CINES), Project No. A0020906873 and the High Performance Computing (HPC) resources of Aix-Marseille University financed by the project Equip@Meso (ANR-10-EQPX-29-01).

References

(1) Hendon, C. H.; Tiana, D.; Walsh, A. Conductive Metal-Organic Frameworks and Networks: Fact or Fantasy? *Phys. Chem. Chem. Phys.* **2012**, *14* (38), 13120–13132. https://doi.org/10.1039/c2cp41099k.

(2) Sun, L.; Campbell, M. G.; Dincă, M. Electrically Conductive Porous Metal-Organic Frameworks. *Angew. Chemie - Int. Ed.* **2016**, *55* (11), 3566–3579. https://doi.org/10.1002/anie.201506219.

(3) Denawi, H.; Abel, M.; Hayn, R. Magnetic Polymer Chains of Transition Metal Atoms and Zwitterionic Quinone. *J. Phys. Chem. C* **2019**, *123*, 4582–4589. https://doi.org/10.1021/acs.jpcc.8b12433.

(4) Leuenberger, M. N.; Loss, D. Quantum Computing in Molecular Magnets. *Nature* **2001**, *410*, 789–793. https://doi.org/10.1038/35071024.

(5) Gaita-arin, A. Mononuclear Lanthanide Single-Molecule Magnets Based on Polyoxometalates. *J. Am. Chem. Soc.* **2008**, *130*, 8874–8875. https://doi.org/10.1021/ja801659m.

(6) Denawi, H.; Koudia, M.; Hayn, R.; Siri, O.; Abel, M. On-Surface Synthesis of Spin Crossover Polymeric Chains. *J. Phys. Chem. C* **2018**, *122* (26), 15033–15040. https://doi.org/10.1021/acs.jpcc.8b04171.

(7) Hurtado Salinas, D. E.; Sarasola, A.; Stel, B.; Cometto, F. P.; Kern, K.; Arnau, A.; Lingenfelder, M. Reactivity of Bioinspired Magnesium–Organic Networks under CO_2 and O_2 Exposure. *ACS Omega* **2019**, *4* (6), 9850–9859. https://doi.org/10.1021/acsomega.9b00762.

(8) Sakamoto, R.; Takada, K.; Sun, X.; Pal, T.; Tsukamoto, T.; Phua, E. J. H.; Rapakousiou, A.; Hoshiko, K.; Nishihara, H. The Coordination Nanosheet (CONASH). *Coord. Chem. Rev.* **2016**, *320–321*, 118–128. https://doi.org/10.1016/j.ccr.2015.12.001.

(9) Grill, L.; Dyer, M.; Lafferentz, L.; Persson, M.; Peters, M. V; Hecht, S. Nano-Architectures by Covalent Assembly of Molecular Building Blocks. *Nat. Nanotechnol.* **2007**, *2*, 687–691. https://doi.org/10.1038/nnano.2007.346.

(10) Barth, J. V.; Costantini, G.; Kern, K. Engineering Atomic and Molecular Nanostructures at Surfaces. *Nature* **2005**, *437* (7059), 671–679. https://doi.org/10.1038/nature04166.

(11) Miner, E. M.; Fukushima, T.; Sheberla, D.; Sun, L.; Surendranath, Y.; Dincə, M. Electrochemical Oxygen Reduction Catalysed by Ni3 (Hexaiminotriphenylene)2. *Nat. Commun.* **2016**, *7*, 1–7. https://doi.org/10.1038/ncomms10942.

(12) Zhao, S.; Wang, Y.; Dong, J.; He, C. T.; Yin, H.; An, P.; Zhao, K.; Zhang, X.; Gao, C.; Zhang, L.; et al. Ultrathin Metal-Organic Framework Nanosheets for Electrocatalytic Oxygen Evolution. *Nat. Energy* **2016**, *1* (12), 16184. https://doi.org/10.1038/nenergy.2016.184.

(13) Ma, T. Y.; Dai, S.; Jaroniec, M.; Qiao, S. Z. Metal-Organic Framework Derived Hybrid Co3O4-Carbon Porous Nanowire Arrays as Reversible Oxygen Evolution Electrodes. *J. Am. Chem. Soc.* **2014**, *136* (39), 13925–13931.

https://doi.org/10.1021/ja5082553.

(14) Clough, A. J.; Yoo, J. W.; Mecklenburg, M. H.; Marinescu, S. C. Two-Dimensional Metal-Organic Surfaces for Efficient Hydrogen Evolution from Water. *J. Am. Chem. Soc.* **2015**, *137* (1), 118–121. https://doi.org/10.1021/ja5116937.

(15) Zhao, D.; Shui, J. L.; Chen, C.; Chen, X.; Reprogle, B. M.; Wang, D.; Liu, D. J. Iron Imidazolate Framework as Precursor for Electrocatalysts in Polymer Electrolyte Membrane Fuel Cells. *Chem. Sci.* **2012**, *3* (11), 3200–3205. https://doi.org/10.1039/c2sc20657a.

(16) Stassen, I.; Burtch, N.; Talin, A.; Falcaro, P.; Allendorf, M.; Ameloot, R. An Updated Roadmap for the Integration of Metal-Organic Frameworks with Electronic Devices and Chemical Sensors. *Chem. Soc. Rev.* **2017**, *46* (11), 3185–3241. https://doi.org/10.1039/c7cs00122c.

(17) Smith, M. K.; Jensen, K. E.; Pivak, P. A.; Mirica, K. A. Direct Self-Assembly of Conductive Nanorods of Metal–Organic Frameworks into Chemiresistive Devices on Shrinkable Polymer Films. *Chem. Mater.* **2016**, *28* (15), 5264–5268. https://doi.org/10.1021/acs.chemmater.6b02528.

(18) Ko, M.; Mendecki, L.; Mirica, K. A. Conductive Two-Dimensional Metal-Organic Frameworks as Multifunctional Materials. *Chem. Commun.* **2018**, *54* (57), 7873–7891. https://doi.org/10.1039/c8cc02871k.

(19) García-Fernández, C.; Sierda, E.; Abadía, M.; Bugenhagen, B.; Prosenc, M. H.; Wiesendanger, R.; Bazarnik, M.; Ortega, J. E.; Brede, J.; Matito, E.; et al. Exploring the Relation between Intramolecular Conjugation and Band Dispersion in One-Dimensional Polymers. *J. Phys. Chem. C* **2017**, *121* (48), 27118–27125. https://doi.org/10.1021/acs.jpcc.7b08668.

(20) Clair, S.; G. de Oteyza, D. Controlling a Chemical Coupling Reaction on a Surface: Tools and Strategies for On-Surface Synthesis. *Chem. Rev.* **2019**, *119*, 4717–4776. https://doi.org/10.1021/acs.chemrev.8b00601.

(21) Koudia, M.; Nardi, E.; Siri, O.; Abel, M. On-Surface Synthesis of Covalent Coordination Polymers on Micrometer Scale. *Nano Res.* **2017**, *10* (3), 933–940. https://doi.org/10.1007/s12274-016-1352-y.

(22) Yang, Q.; Siri, O.; Braunstein, P. First Transamination Reactions for the One-Pot Synthesis of Substituted Zwitterionic Quinones. *Chem. Commun.* **2005**, *5*, 2660–2662. https://doi.org/10.1039/b501926e.

(23) Siri, O.; Braunstein, P. Unprecedented Zwitterion in Quinonoid Chemistry. *Chem. Commun.* **2002**, *2* (3), 208–209. https://doi.org/10.1039/b107828n.

(24) Truhlar, D. G. Ab- initio Simulations of Materials Using VASP: Density- functional Theory and Beyond. *J. Comput. Chem.* **2008**, *29*, 2044–2078. https://doi.org/10.1002/jcc.

(25) Kresse, G.; Furthmüller, J. Efficient Iterative Schemes for Ab Initio Total-Energy Calculations Using a Plane-Wave Basis Set. *Phys. Rev. B - Condens. Matter Mater. Phys.* **1996**, *54* (16), 11169–11186. https://doi.org/10.1103/PhysRevB.54.11169.

(26) Kresse, G.; Joubert, D. From Ultrasoft Pseudopotentials to the Projector Augmented-Wave Method. *Phys. Rev. B - Condens. Matter Mater. Phys.* **1999**, *59* (3), 1758–1775. https://doi.org/10.1103/PhysRevB.59.1758.

(27) Perdew, J. P.; Chevary, J. A.; Vosko, S. H.; Jackson, K. A.; Pederson, M. R.; Singh, D. J.; Fiolhais, C. Erratum: Atoms, Molecules, Solids, and Surfaces: Applications of the Generalized Gradient Approximation for Exchange and Correlation. *Phys. Rev. B.* 1993, p 4978. https://doi.org/10.1103/PhysRevB.48.4978.2.

(28) J.P.Perdew; Y.Wang. Accurate and Simple Analytic Representation of the Electron-Gas Correlation Energy. *Phys. Rev. B* **1992**, *45* (23), 13244–13249. https://doi.org/10.1103/PhysRevB.45.13244.

(29) Blöchl, P. E. Projector Augmented-Wave Method. *Phys. Rev. B* **1994**, *50* (24), 17953–17979. https://doi.org/10.1103/PhysRevB.50.17953.

(30) Kresse, G.; Furthmiiller, J. Efficiency of Ab-Initio Total Energy Calculations for Metals and Semiconductors Using a Plane-Wave Basis Set. *Comput. Mater. Sci.* **1996**, *6*, 15–50. https://doi.org/10.1002/j.1551-8833.2007.tb07844.x.

(31) A. I. Liechtenstein, V. I. A.; J. Zaanen. Density-Functional Theory and Strong Interactions: Orbital Ordering in Mott-Hubbard Insulators. *Phys. Rev. B* **1995**, *52* (8), 5467–5471. https://doi.org/10.1103/PhysRevB.52.R5467.

(32) Mabrouk, M.; Hayn, R.; Denawi, H.; Ben Chaabane, R. Possibility of a Ferromagnetic and Conducting Metal-Organic Network. *J. Magn. Magn. Mater.* **2018**, *453* (May), 48–52. https://doi.org/10.1016/j.jmmm.2018.01.005.

(33) Zhou, J.; Sun, Q. Magnetism of Phthalocyanine-Based Organometallic Single Porous Sheet. *J. Am. Chem. Soc.* **2011**, *133* (38), 15113–15119. https://doi.org/10.1021/ja204990j.

(34) Pack, J. D.; Monkhorst, H. J. Special Points for Brillouin-Zone Integrations. *Phys. Rev. B* **1976**, *13*, 5188−5192. https://doi.org/10.1103/PhysRevB.16.1748.

TOC Graphic